Recombination processes in SiGe/Si quantum wells measured by photoinduced absorption spectroscopy

E. Dekel, E. Ehrenfreund, and D. Gershoni

Department of Physics and Solid State Institute, Technion-Israel Institute of Technology, Haifa 32000, Israel

P. Boucaud

Institut d'Electronique Fondamentale, URA 22 CNRS, Université Paris XI, F-91405 Orsay, France

I. Sagnes and Y. Campidelli

France Telecom, CNET-CNS Boîte Postale 98, F-38243 Meylan, France

We used photoinduced absorption spectroscopy of optical transitions between valence subbands of nominally undoped SiGe/Si quantum wells to study the recombination processes of photogenerated carriers in these heterostructures. We measured the photoinduced absorption as a function of the ambient temperature, photoexcitation density, and modulation frequency. The energy band structure of the SiGe/Si quantum well and the optical transitions between its valence subbands are calculated using an eight-band $\mathbf{k}\cdot\mathbf{p}$ model. The model, which includes sets of bulk Si and Ge parameters, agrees very well with the observed intersubband transition and its magnitude. Thus, the photoinduced absorption intensity is a direct measure of the photogenerated excess carrier density, for which we measured a characteristic time scale for a decay of $\simeq 2.5$ μsec at 80 K, and longer times at lower temperatures. Our measurements show that the recombination kinetics is governed by both an extrinsic monomolecular and intrinsic bimolecular terms. We incorporate this density dependence into a simple rate model that takes into account thermal activation of the photogenerated holes out of the SiGe quantum wells. The model describes very well the measured temperature dependence of the photoinduced absorption and it provides quite an accurate determination of the intrinsic recombination rate of electrons and holes within the well regions in these heterostructures. The rate that we obtain is faster than the measured recombination rates in bulk Si and Ge. We believe that this recombination rate enhancement is due to carriers confinement within the SiGe quantum-well regions. [S0163-1829(97)06447-3]

I. INTRODUCTION

In recent years Si/Ge quantum heterostructures have attracted considerable attention due to the extensive progress in the growth technology, the considerable improvement in heterostructures quality, and their potential compatibility with the silicon-based electronic industry. Two main features characterize this important semiconductor material system. The first feature is the indirect energy gap of both Si and Ge. The second one is the distribution of the band-gap energy difference between the two materials, which takes place mostly within the valence bands. Thus, in a typical $Si_{1-x}Ge_x$/Si heterostructure interface the indirect conduction-band bottom from both sides of the interface are nearly aligned, and the valence bands are considerably offset.[1]

Due to the indirect nature of the band structure, direct radiative recombination of photoexcited carriers is prohibited, resulting in a relatively weak and long-lived photoluminescence (PL) emission from photoexcited SiGe quantum structures. Therefore, there is an obvious advantage in studying these structures using photoinduced absorption spectroscopy in which optical transitions of holes between their valence subbands are probed following their photoexcitation, rather than the PL.

We applied this technique to study the relaxation of photogenerated holes in the valence band of SiGe quantum structures. We measured the intersubband photoinduced absorption (PIA) as a function of the excitation density, modulation frequency, and sample temperature.

We used an eight-band $\mathbf{k}\cdot\mathbf{p}$ model in order to calculate the intersubband absorption spectrum in this indirect material. The eight bands used are the three doubly degenerated valence bands (heavy hole, light hole, and split off bands) and the lowest direct, Γ-point conduction band. By applying this model to the structure under study, we explain the measured valence intersubband absorption magnitude, and its spectral shape and position.

In Sec. II we describe the studied heterostructures and the experimental setup. In Sec. III we present the experimental measurements, which we discuss and analyze in Sec. IV. Section V is a short summary of our study.

II. SAMPLES AND EXPERIMENT

The Si/Ge quantum well (QW) studied here was grown by ultrahigh-vacuum chemical-vapor deposition using a Riber Epineat growth chamber on undoped (100)-oriented Si substrate. The structure is composed of 50 periods of 20-Å $Si_{0.7}Ge_{0.3}$ wells separated by 170-Å Si barriers. In order to allow intersubband absorption measurements in both s- and p-polarization configurations, the sample was prepared as a multipass waveguide by polishing two parallel cleavage facets at a 45° angle (see inset Fig. 1).

All measurements were done using a Bruker IFS66V Fourier-transform infrared (FTIR) spectrometer equipped
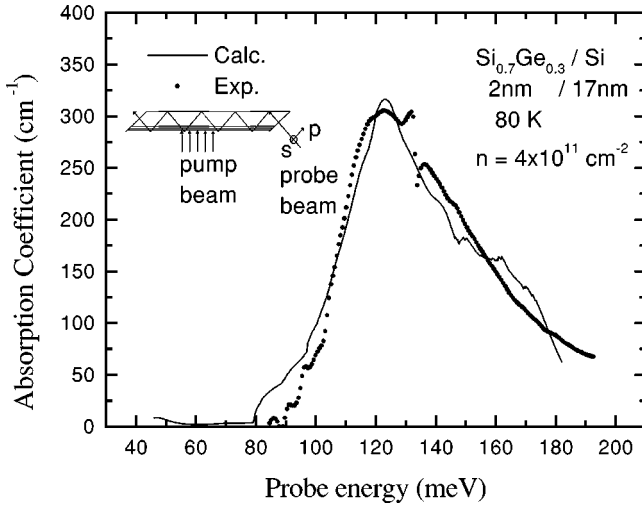
FIG. 1. Measured p-polarized ($\bullet$), and calculated (solid line) photoinduced absorption spectra for 20-Å/170-Å $Si_{0.7}Ge_{0.3}$/Si strained layer superlattice at 80 K. The photoexcited carrier density per period is $\simeq 4 \times 10^{11}$ cm^{-2}. The absorption coefficient was extracted from the measured $-\Delta T/T$ by taking into account the waveguide geometry, the pump beam spot size, and the number of periods. The inset describes schematically the experimental layout.

with a step-scan mirror movement to allow pump beam modulation using conventional lock-in techniques. The 514.5-nm Ar$^+$ line pump laser beam was modulated by an acousto-optic modulator operating in the range 10 Hz to $\simeq 2$ MHz. The probe beam, an incandescent Nernst glower, was detected using a mercury cadmium telluride detector. The modulation technique allows us to study the recombination processes for the photoexcited carriers by varying the pump laser beam intensity and modulation frequency and by varying the temperature. Although similar results could be obtained by measuring the transients of the photoinduced absorption, the modulation technique better fits our step-scan FTIR spectrometer. In each polarization, both the transmission T and the photoinduced changes ΔT were measured, and the results are presented as $-\Delta T/T$, which is the photoinduced absorbance. In the s-polarization geometry, the electric field (E) of the infrared (IR) radiation, propagating along the waveguide, has no component along the QW growth direction (z axis). In the p-polarization geometry the IR electric field is equally divided between the z axis and the x-y plane (see inset, Fig. 1). Since in this work the PIA is used as a measure for the excess carriers density, we report on measurements performed using the latter geometry only.

III. RESULTS

Figure 1 displays the PIA measurements for the p polarizations in the energy range 0.08–0.2 eV at $\simeq 80$ K and at pump intensity of $\simeq 3$ W/cm^2. In the p-polarization geometry (solid circles) a strong PIA band centered around 0.125 eV is apparent. (The sharp feature at $\simeq 0.14$ eV is probably due to the surface oxide layer[2].) Comparison with our model calculations, as we show here, indicates that this transition is actually an optical transition from the HH1 subband to the valence-band continuum, in agreement with Ref. 2.

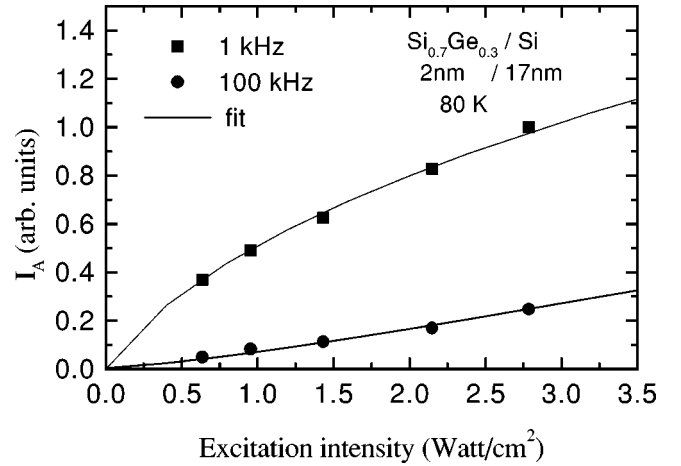Figure 2 shows the dependence of the in-phase compo-

FIG. 2. The integrated PIA intensity I_A as a function of the laser excitation intensity I_L, at $\nu=1$ kHz ($\blacksquare$) and $\nu=100$ kHz ($\bullet$) modulation frequencies and at 80 K. The solid lines represent best fits to the quadratic rate equation [Eq. (1)].

nent of the integrated p-polarized PIA intensity, $I_A \equiv \int(-\Delta T/T)d\epsilon$, on the exciting laser intensity, I_L, for two modulation frequencies, $\nu=1$ and 100 kHz. It is interesting to note that, at these two frequencies, the I_L dependence is markedly different. Whereas, at 100 kHz, I_A is nearly linear with I_L, at 1 kHz it is sublinear ($I_A \propto I_L^\gamma$, with $\gamma \simeq 0.5$). Below we will show that this behavior is expected for a recombination process with quadratic dependence on the photogenerated carriers density.

The dependence of I_A on ν is shown in Fig. 3 for both the in-phase and out-of-phase components, in the range 1–150 kHz at 80 K. The out-of-phase component has a peak at $\simeq 62$ kHz, where the in phase component is reduced approximately by a factor of 2 from its low-frequency value. It means that an ''average'' time of $\simeq 2.5$ μsec characterizes the HH recombination process at this temperature. At 5 K this characteristic time is about four times longer.

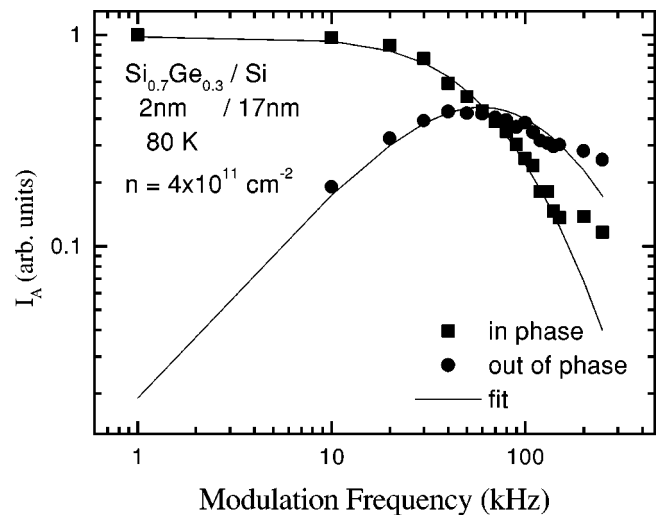FIG. 3. The integrated PIA intensity I_A as a function of the excitation modulation frequency ν for the in-phase ($\blacksquare$) and out-of-phase ($\bullet$) components, at 80 K and excitation density of $\simeq 4 \times 10^{11}$ per cm^2 per period. The solid lines represent best fits to the quadratic rate equation [Eq. (1)]. Note the log-log scale.
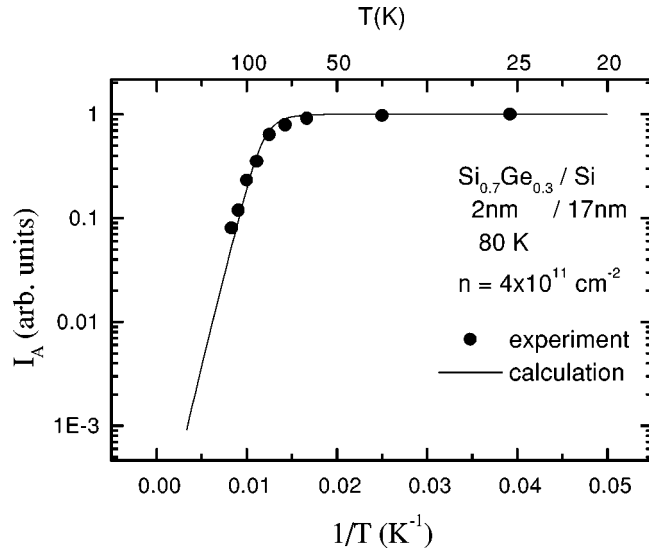
FIG. 4. Arrhenius plot of the integrated PIA, I_A, measured at a modulation frequency of 1 kHz and pump intensity of $I_L \simeq 3$ W/cm^2 ($\bullet$). The solid line is the calculated temperature dependence using Eq. (7).

Figure 4 shows the temperature dependence of I_A in the range 5–150 K. A sharp drop of the photoinduced absorption is apparent above $\simeq 70$ K, indicating an activation like recombination process.

IV. DISCUSSION

A. PIA spectra

Absorption, unlike photoluminescence, directly measures the density of the absorbing species, and it can be readily interpreted quantitatively. For a quantitative analysis of the valence intersubband photoinduced absorption, a preliminary knowledge of the subbands dispersion and the matrix elements for optical transitions between them is required. It is well known that one of the best ways to quantitatively model the optical properties of semiconductor heterostructures is by the use of a multiband envelope function and the $\mathbf{k} \cdot \mathbf{p}$ approximations.[3] Models based on these approximations are routinely and most successfully applied to III-V compound heterostructures.[4,5] Since most of the III-V compounds are direct, the inclusion of the lowest Γ conduction band in these models is natural and self-evident. For indirect materials,

such as silicon and germanium, this is not obvious, and usually the direct conduction band (Γ) is treated as a remote band that is not included within the multiband model.[3,6] Unfortunately, this is not possible when the quantitative modeling of direct optical transitions is required. For this case the direct s-symmetry Γ conduction band must be included within the multiband set, since it is its interaction with the valence bands that determines the intensity of all optical transitions. We emphasize here that even for the calculations of *valence* intersubband optical absorption strength the direct conduction band must be included in the multiband model. For our calculations we use the model that was introduced by Gershoni, Henry, and Baraff.[5] This $\mathbf{k} \cdot \mathbf{p}$ model uses eight-band envelope functions and bulk material parameters. The effects of the lattice mismatch strain are incorporated into the model using bulk deformation potentials. The main problem in applying such an eight-band model to indirect materials such as Si and Ge is the uncertainty in the material parameters associated with the direct conduction band. These parameters cannot be easily determined by optical measurements and, therefore, they are not well documented. We thus tried to obtain a set of Ge and Si material parameters from reliable literature sources. A list of all the parameters used in our model are given in Table I. We checked the internal consistency of these material constants by an attempt to reproduce by calculations a large set of published experimental results.[1,7] We succeeded in finding a set of such parameters that enable us to account for many PL (Refs. 8 and 9) and inter-sub-valence-band absorption data.[2,6,10,11] We note here that another useful way to calculate the sub-valence-band structure and intersubband absorption in indirect QW's is the empirical pseudopotential method used previously for SiGe/Si heterostructures.[12]

The calculated energies of the highest Γ valence subbands are plotted in Fig. 5 as a function of the in-plane crystal momentum $\mathbf{k}_\parallel$ along the (010) direction. The confined energy levels are identified according to the number of nodes in their wave functions and their total angular momentum projection along the growth direction at $k_\parallel = 0$. They are marked on the figure as either heavy holes (M$_J=3/2$) or light holes (M$_J=1/2$). It is seen that only a single HH and a single LH levels are strictly confined to the SiGe layer. The third valence subband is already a miniband in the continuum above the top of the QW.

The matrix elements for optical transitions between the various subbands are calculated using the dipole approxima-

TABLE I. Constants used in the band-structure calculations. γ_1, γ_2, and γ_3 are the Luttinger parameters and E_P is the optical transition matrix element (expressed in eV) (Refs. 3 and 4). m_e is the bulk electron mass given as a fraction of the free-electron mass m. Δ_{so} is the split off energy, $E_{g,d}$ is the direct band gap at the Γ point, V_{off} is the offset energy. a_V and a_g are the hydrostatic strain potentials for the valence band and the total gap, respectively, b_V is the valence-band shear deformation potential, and c_{11} and c_{12} are the relevant elastic constants (given in Mbar units).

	E_P eV (Ref. 26)	γ_1 (Ref. 7)	γ_2 (Ref. 7)	γ_3 (Ref. 7)	m_e (Ref. 27)	Δ_{so} meV (Ref. 7)	$E_{g,d}$ eV (Ref. 7)	V_{off} meV (Ref. 28)	a_V eV (Ref. 28)	a_g eV (Ref. 1)	b_V eV (Ref. 1)	c_{11} Mbar (Ref. 1)	c_{12} Mbar (Ref. 1)
Si	21.6	4.285	0.339	1.446	0.528	44	4.185	0^a	0^a	1.72	−2.1	1.675	0.650
Ge	26.3	13.38	4.240	5.69	0.038	297	0.898	530^a	0^a	−2.8	−2.9	1.315	0.494

$^a a_V$ is chosen arbitrarily as zero. The effect of the hydrostatic strain is incorporated into the offset values V_{off}.
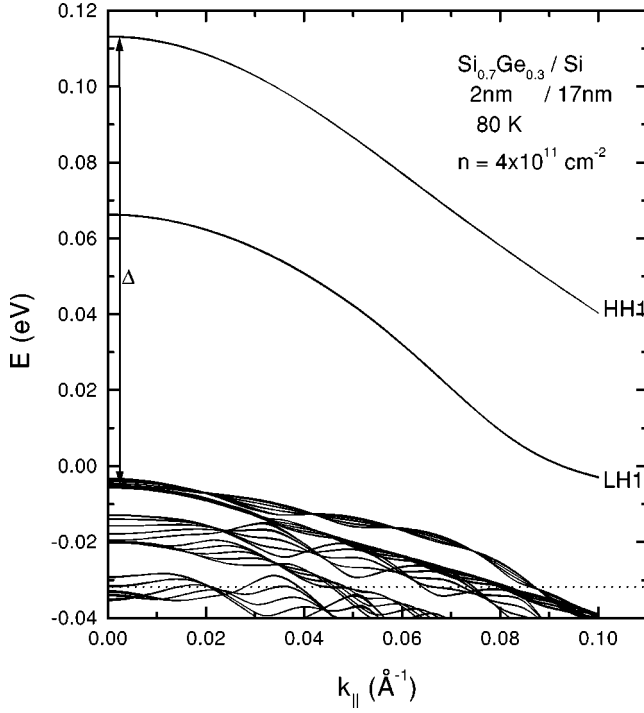
FIG. 5. The calculated valence band dispersion relation for 20/170- Å $Si_{0.7}Ge_{0.3}$/Si strained-layer superlattice, plotted as energy vs in-plane wave vector, $k \parallel 100$. The energy is measured relative to the top of the Si barrier valence band.

tion and the calculated wave functions.[5] The absorption calculations are then performed by using the experimentally estimated steady-state hole density ($\simeq 2 \times 10^{18}$ cm^{-3}) and assuming thermal equilibrium. The calculated intersubband absorption spectrum for the p polarization is displayed in Fig. 1 as a solid line. It is seen that the magnitude, spectral position, and spectral line shape of the measured PIA is well reproduced by our model calculations. [The calculated PIA magnitude agrees, within the uncertainties involved in the estimated density of photoinduced holes ($\simeq 50\%$), with the measured PIA magnitude.] The relatively large line width is the result of the transitions from the confined HH1 subband to the minibands at the onset of the heterostructure continuum,[13] as can be seen in Fig. 5. We note here that the spectral position of the measured and calculated PIA occurs at 125 meV, this agrees also with the simpler model calculations of Ref. 2.

B. Recombination kinetics

The sublinear (nearly square-root) excitation density dependence of the PIA as clearly observed at low modulation frequencies (Fig. 2) is a clear evidence for the presence of a quadratic density term in the recombination kinetics. We have, therefore, fitted our data to the simplest nonmonomolecular recombination kinetic equation:

$$d\rho/dt = g(t) - \alpha\rho - \beta\rho^2, \quad (1)$$

where ρ is the photoexcited excess carriers density, α and β are rate constants that are independent of ρ, and $g(t)$ is the time-dependent carrier photogeneration rate. In our experiment, $g(t)$ is proportional to the intensity of the modulated

pump beam and thus given by $g(t) = g(1 + \cos 2\pi\nu t)/2$, where the constant g contains in it the quantum efficiency for carriers photogeneration and ν is the modulation frequency. We have numerically solved Eq. (1) for ρ as a function of the modulation frequency and laser intensity, and fitted the solutions to the experimental data. The continuous lines in Fig. 2 and Fig. 3 are the best fits to the measured data. For these fits we have found $\alpha = 1.3 \times 10^5$ sec^{-1} and $\beta = 9 \times 10^{-14}$ cm^3 sec^{-1}.

The very good fits obtained show that the measured data are well described by Eq. (1). We note in particular, that our kinetic model accounts very well for the nearly square-root excitation density dependence of the PIA at low modulation frequencies, and its almost linear dependence at high modulation frequencies. This behavior is characteristic of quadratic rate equations, as already noted previously.[14] Since the rate equation is not linear in ρ, the definition of a photogenerated population lifetime is not so straightforward as it is in the linear case. We choose to define a characteristic time scale for the population lifetime as the inverse of the frequency where the out of phase component of the measured PIA reaches its maximum (Fig. 3). In the linear case, this choice of time scale is equivalent to the time it takes for a certain carrier density generated by a short impulse to decay to $1/e$ that density. As can be seen in Fig. 3, this characteristic time scale is $(2\pi \times 62$ kHz$)^{-1} = 2.5$ μsec.

C. The recombination mechanism

Important recombination mechanisms in indirect bulk semiconductors are processes in which intermediate trap levels are involved.[15] In bulk Si, for instance, the impurity dominated Auger process gives rise to low temperature carrier lifetimes in the range of 1 ns–1 μs,[16,17] depending on the binding energy of the impurity. Many studies of the recombination statistics of these processes in bulk indirect semiconductors were analyzed in detail in the literature.[15,17–19] A common feature to all these processes is the saturation of the recombination as the photoinduced carrier density exceeds the trap density. In our quantum-well structures, the steady state photoinduced carrier density within the quantum wells exceeds 10^{18} cm^{-3}. This is considerably denser than any possible concentration of impurities or traps in this nominally undoped sample. Yet, we observed no saturation of the absorption as the pump power increases. In our case we can, thus, safely ignore impurity- and trap-related recombination processes within the quantum wells. These relatively fast processes, however, must be considered for carrier recombination within the silicon barriers of the heterostructure, since the density of thermally activated carriers within them is orders of magnitude lower. A completely different model, namely, intrinsic Auger recombination via HH and LH minibands, was suggested for p-type SiGe/Si heterostructures.[12]

Our model is similar, in principle, to the model of Michler et al.,[20] which assumes thermal equilibrium between carriers in the quantum-well regions and in the barrier regions during the recombination process. This thermal equilibrium is due to a fast forward-backward scattering between the quantum wells and barriers; see Fig. 6.

Our model is different from that of Ref. 20 in its recombination kinetics. We assume that the recombination is gov-
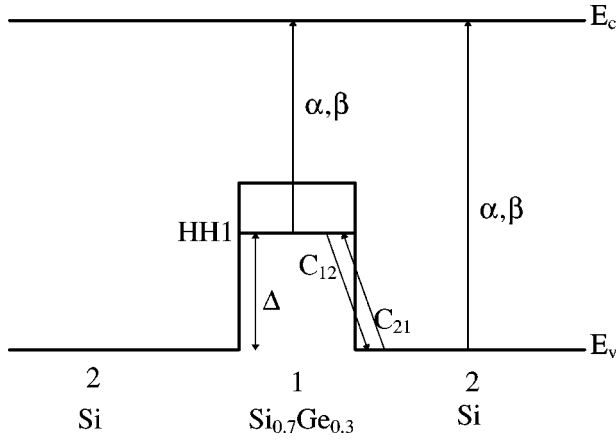
FIG. 6. Schematic description of the recombination processes of the photoexcited carriers in the strained-layer superlattice. α and β are the monomolecular and bimolecular recombination coefficients, respectively, and C_{12} and C_{21} are the scattering rates between well (region 1) and barrier (region 2) states.

erned by two processes. The first is extrinsic and depends on the density of the extrinsic recombination centers within the material, N_0. This process is thus, monomolecular in nature, and it is saturated once the density of excess carriers ρ exceeds N_0, which is estimated to be $10^{15}-10^{16}$ cm^{-3}. The second process is intrinsic and is characteristic of the material itself. It is, thus, bimolecular in nature.[18,19] Since the barriers and wells in our heterostructure differ only by their germanium content, we assume for simplicity that the recombination rate U in both materials can be described in the same way:

$$U = A(1 - \rho/N_0)\Theta(1 - \rho/N_0)\rho + B\rho^2, \qquad (2)$$

where N_0, the density of the extrinsic nonradiative recombination centers, is assumed to be uniform throughout the entire heterostructure, Θ is a step function, and A and B are the rates for the extrinsic and intrinsic processes, respectively. As discussed above, it is imperative to note that the extrinsic process in the rate equation causes the recombination rate within the quantum wells to be vastly different from that in the barriers. This is because at low temperatures the steady-state carrier density in the well regions is much higher than N_0, while the density of carriers within the barriers is considerably lower than N_0.

Based on the above assumptions we write the rate equations for the photoexcited heavy holes in the two regions

$$\frac{d\rho_i}{dt} = g_i - U_i - (-1)^i C_{21}p_2 + (-1)^i C_{12}p_1 \quad (i = 1,2),$$
$$(3)$$

where $i = 1,2$ refers to the well and barrier, respectively, $p_i = p_{iG} + \rho_i$ $(i = 1,2)$ are the total nonequilibrium hole densities, and p_{iG} is the (dark) thermal equilibrium hole density. g_i is the generation rate of holes and electrons in each of the regions.

Under thermal equilibrium conditions, the rates C_{ij} can be directly related to the densities p_{iG}: $C_{21}/C_{12} = p_{1G}/p_{2G}$, and the ratio ρ_2/ρ_1 is readily obtained as

$$\rho_2/\rho_1 = C\sqrt{T}\exp(-\Delta/2k_BT), \qquad (4)$$

where Δ is the sum of the electron and hole well to barrier activation energies, and the constant C can be expressed as $C = (m_{n2}m_{p2})^{3/4}(m_{n1}m_{p1})^{-1/2}(2\pi k_B)^{1/2}L_z/h$ if one uses the parabolic band approximation.[20] (m_{ni}, m_{pi} are the electron and hole masses, respectively, in the two regions). In obtaining Eq. (4), a 2D (3D) density of states was assumed in the well (barrier) region. (We note here that even if the electrons are not confined to the well region by the conduction-band offset, neutrality still imposes their 2D behavior.)

For the densities relevant to our experiment we can safely assume $p_{2G} < N_0 < p_{1G}$ and $\rho_i \gg p_{iG}$ $(i = 1,2)$. Thus, the recombination is trap limited only in the barrier region, and in both regions the photoinduced carrier density is much higher than the equilibrium dark carrier density. Under these conditions, we obtain, for the heavy-hole density in the well region,

$$d\rho_1/dt = g - \alpha(T)\rho_1 - \beta(T)\rho_1^2, \qquad (5)$$

with

$$\alpha(T) = AC\sqrt{T}\exp(-\Delta/2k_BT),$$

$$\beta(T) = B(1 + C^2T\exp(-\Delta/k_BT)). \qquad (6)$$

In the present case, the conduction-band offset is nearly zero. Thus, Δ is in effect the energy separation between the HH1 level and the top of the barrier valence band.

From Eq. (6) and the experimentally determined values of α and β at $T = 80$ K, the rate constants A and B can be uniquely found. We find $A^{-1} \simeq 10$ nsec, and $B \simeq 9 \times 10^{-14}$ cm^3 sec^{-1}, respectively. The inverse extrinsic rate A is comparable with measured impurity mediated Auger recombination lifetimes in bulk Si.[16,17] The intrinsic rate B, which is a fundamental property of these indirect semiconductors, is somewhat higher than the range of the reported measured values for bulk Si [$(1-6) \times 10^{-14}$ cm^3 sec^{-1} (Refs. 21–23)], and the calculated recombination rate of Ge [$B \simeq 3 \times 10^{-14}$ cm^3 sec^{-1} (Ref. 24)]. We believe that this enhancement in the intrinsic recombination rate of carriers within the Ge$_x$Si$_{1-x}$ layers is a consequence of the quantum confinement. Similar enhancement is known to occur in direct-band-gap heterostructures.[25]

A posteriori, we note here that the assumption $\rho_1 \gg N_0 \gg \rho_2$ is well justified, since the photoinduced density of holes in the well is $\rho_1 \simeq 2 \times 10^{18}$ cm^{-3} and $\rho_2/\rho_1 = C\sqrt{T}\exp(-\Delta/2k_BT) \simeq 3 \times 10^{-4}$ at $T = 80$ K.

Under steady-state conditions ($d\rho_1/dt = 0$), the density of the photogenerated excess carriers in the well is given by

$$\rho_1(T) = \frac{\alpha(T)}{2\beta(T)}\left\{\left[1 + \frac{4g\beta(T)}{\alpha(T)^2}\right]^{1/2} - 1\right\}. \qquad (7)$$

Since the photoinduced intersubband absorption signal is a direct measure of the density of heavy holes in the well, Eq. (7) describes the PIA intensity under steady-state conditions. We have, thus, calculated the temperature dependence of the steady-state excess carrier density within the well, $\rho_1(T)$, using Eqs. (6) and (7) and the calculated values for $\Delta = 125$ meV (see Sec. IV A) and $C \simeq 0.1$ K$^{-1/2}$ (see Sec. IV C and Table I). The result of this calculation (with no adjustable parameters) is given by the solid line in Fig. 4. As can be

seen, the model describes very well the measured data. We note, in particular, that the calculated $\Delta = 125$ meV agrees very well with the observed activation energy. In this respect, it is interesting to compare our results with previous activation energy measurements of the PL recombination process in SiGe/Si heterostructures.[29] In this work, the PL dependence on temperature was interpreted as due to activation over the energy barrier for holes, similar to our finding.

V. SUMMARY

We have studied the recombination of photogenerated carriers in SiGe/Si quantum-well by measuring the photoinduced intersubband absorption for various temperatures, laser intensities and modulation frequencies. We have used an eight-band $\mathbf{k} \cdot \mathbf{p}$ model to calculate the sub-valence-band structure and the inter-sub-valence-band optical matrix elements. Using bulk material parameters we have calculated the intersubband optical absorption and found good agreement with the experimental measurements. In particular, we have shown that the intersubband absorption strength is a reliable direct measure of the hole density within the heterostructure.

From the excitation density and modulation frequency dependence of the photoinduced intersubband absorption we have shown that up to carrier densities of few times 10^{18} cm^{-3}, the recombination rate can be described by a sum of monomolecular and bimolecular terms. From the temperature dependence of the PIA, which has an activation-like behavior with characteristic energy of half the calculated holes confinement energy, we have deduced that thermionic emission of holes maintains thermal equilibrium of carriers within the heterostructure.

These observations are very well explained by an assumption that the monomolecular term in the recombination rate is due to extrinsic nonradiative recombination centers. Within the SiGe well regions, the density of excess carriers far exceeds the density of these extrinsic centers, while within the Si barrier regions the density of excess carriers is much lower than the density of the extrinsic centers. Thus, within the wells, the recombination is intrinsic, bimolecular in nature, and in the barriers it is extrinsic, monomolecular in nature. From our data we have quite accurately calculated the intrinsic recombination rate of carriers in SiGe quantum wells. The rate that we have obtained, which is slightly higher than the measured rates in both bulk Si and bulk Ge, suggests an enhancement in the recombination rate due to carrier quantum confinement.

[1] C.G. van de Walle, Phys. Rev. B **39**, 1871 (1989).

[2] P. Boucaud, L. Wu, Z. Moussa, F. H. Julien, J.-M. Lourtioz, I. Sagnes, Y. Campidelli, and P.-A. Badoz, Superlattices Microstruct. **19**, 33 (1996).

[3] E. O. Kane, J. Phys. Chem. Solids **1**, 249 (1957).

[4] G. Bastard, *Wave Mechanics Applied to Semiconductor Heterostructures* (Les Editions de Physique, Les Ulis, France, 1988).

[5] D. Gershoni, C. H. Henry, and G. A. Baraff, IEEE J. Quantum Electron. **29**, 2433 (1993).

[6] T. Fromherz, E. Koppensteiner, M. Helm, G. Bauer, J. F. Nützel, and G. Abstreiter, Phys. Rev. B **50**, 15 073 (1994).

[7] *Intrinsic Properties of Group IV Elements and III-V, I-VII Compounds,* edited by O. Madelung, M. Schulz, and H. Weiss, Landolt–Bornstein, New Series, Group III, Ch. B.1.2 (Springer-Verlag, Berlin, 1985), Vol. 22a.

[8] J. C. Sturm, H. Manoharan, and L. C. Lenchyshyn, Phys. Rev. Lett. **66**, 1362 (1991).

[9] S. Fukatsu, H. Yoshidu, and F. Fujiwava, Appl. Phys. Lett. **61**, 804 (1992).

[10] L. Wu, P. Boucaud, J. M. Lourtioz, F. H. Julien, I. Sagnes, Y. Campidelli, and P.-A. Badoz, Appl. Phys. Lett. **67**, 3462 (1995).

[11] P. Boucaud, L. Gao, Z. Moussa, F. Visocekas, F. H. Julien, J.-M. Lourtioz, I. Sagnes, Y. Campidelli, and P.-A. Badoz, Appl. Phys. Lett. **67**, 2948 (1995).

[12] E. Corbin, C. J. Williams, K. B. Wong, R. J. Turton, and M. Jaros, Superlattices Microstruct. **19**, 25 (1996).

[13] D. Gershoni, J. Oiknine-Schlesinger, E. Ehrenfreund, D. Ritter, R. A. Hamm, and M. B. Panish, Phys. Rev. Lett. **71**, 2975 (1993).

[14] C. Botta, S. Luzzati, R. Tubino, D. D. C. Bradley, and R. H. Friend, Phys. Rev. B **48**, 14 809 (1993).

[15] W. Shockley and W. T. Read, Phys. Rev. **87**, 835 (1952).

[16] S. A. Lyon, G. C. Osburn, D. L. Smith, and T. C. McGill, Solid State Commun. **23**, 425 (1977).

[17] W. Schmid, Phys. Status Solidi B **84**, 529 (1977).

[18] J. I. Pankove, *Optical Processes in Semiconductors* (Dover, New York, 1975), Chap. 6.

[19] J. S. Blakemore, *Semiconductor Statistics* (Dover, New York, 1987), Chap. 6.

[20] P. Michler, A. Hangleiter, M. Moser, M. Geiger, and F. Scholz, Phys. Rev. B **46**, 7280 (1992).

[21] L. M. Blinov, E. A. Bobrova, V. S. Vavilov, and G. N. Galkin, Fiz. Tverd. Tela (Leningrad) **9**, 3221 (1967) [Sov. Phys. Solid State **9**, 2537 (1967)].

[22] W. Michaelis and M. H. Pilkuhn, Phys. Status Solidi **36**, 311 (1969).

[23] W. Gerlach, H. Schlangenotto, and H. Maeder, Phys. Status Solidi A **13**, 277 (1972).

[24] W. van Roosbroeck and W. Shockley, Phys. Rev. **94**, 1558 (1954).

[25] B. Sermage, D. S. Chemla, D. Sivco, and A. Y. Cho, IEEE J. Quantum Electron. **22**, 774 (1986).

[26] R. L. Aggarwal, Phys. Rev. B **2**, 446 (1970).

[27] C. Tserbak, H. M. Polatoglou, and G. Theodorou, Phys. Rev. B **47**, 7104 (1993).

[28] C. G. van de Walle, and R. M. Martin, Phys. Rev. B **34**, 5621 (1986).

[29] J. C. Sturm, A. S. Amour, Q. Mi, L. C. Lenchyshyn, and M. L. W. Thewalt, Jpn. J. Appl. Phys. **33**, 2329 (1994).